Stability and Conformation of Polycopper−Thiolate Clusters Studied by Density Functional Approach

Priit Ahte, Peep Palumaa, and Toomas Tamm*

Faculty of Natural Sciences, Tallinn University of Technology, Tallinn, Estonia

Received: December 29, 2008; Revised Manuscript Received: May 8, 2009

Quantum chemical studies of biologically relevant copper thiolate clusters can afford unique information about energetic principles of their formation and structure, which is important for understanding the basic principles of their formation and functioning in biological systems. In the current study, we used quantum chemical methods for the investigation of the structure and stability of Cu_xS_y-type clusters that serve as models for different copper thiolate clusters or for their intermediates in a variety of copper proteins. Density functional theory based modeling was performed including solvent effects for water and protein-like environments. Thermodynamic parameters (ΔH, ΔS, ΔG) were calculated in order to assess the effect of thermal contributions to the formation energies of various copper thiolate clusters. The all-tricoordinated polycopper thiolate cluster $[Cu_4(SMe)_6]^{2-}$ turned out to be the most stable structure among the calculated ones. This result is in agreement with the prevalence of this type of clusters in various copper proteins with no sequence homology that contain six cysteine residues. The cooperativity of formation of $[Cu_4(SMe)_6]^{2-}$ can be inferred from the significant energy differences between intermediary clusters. Among tetrathiolate structures, $[Cu_2(SMe)_4]^{2-}$ was the most stable one. This cluster is also found in many copper proteins. Influence of slight structural perturbations on the energetics of copper thiolate clusters is also analyzed and discussed.

Introduction

Copper is an essential microelement, biological handling of which is almost exclusively protein-mediated. Many proteins participating in cellular transport or storage of Cu(I) ions form polynuclear Cu(I) thiolate clusters. The most common biological motifs involved in these processes are tetracopperhexathiolate and dicoppertetrathiolate clusters. However, larger clusters also occur.

Tetracopperhexathiolate clusters are formed in a variety of functionally different proteins like yeast copper sensor Ace1,[1] copper chaperone for cytochrome-*c* oxidase Cox17,[2] copper chaperone for Zn, CuSOD denoted Ccs,[3] C-terminal cytosolic part of yeast copper influx transporter Ctr1,[4] and yeast copper ATPase denoted Ccc2,[4] as well as by mammalian copper ATPases ATP7A and ATP7B.[5,6] Polycopper thiolate clusters have been demonstrated to occur also in metallothioneins (MTs), Cys-rich low-molecular-weight proteins involved in the metabolism of zinc and copper and in detoxification of Cd(II) ions.[7] Mammalian MTs form two Cu(I) thiolate clusters, which are tetracopper thiolate clusters according to spectroscopic evidence.[8−11] Yeast MT, denoted Cup1, differs from mammalian MTs by forming one octacopperdecathiolate (Cu_8S_{10})-type cluster, which is the largest known oligonuclear Cu(I) thiolate cluster in a biological system.[12]

It follows that tetracopper thiolate clusters are formed by functionally diverse proteins, which participate in various steps of intracellular copper metabolism. A prerequisite for tetracopper cluster formation is the presence of six or more Cys residues that can be located either within a relatively short polypeptide sequence in a single protein domain (MTs, Ace1, Cox17, Ctr1, Ccs2) or in different structural domains (Ccs, ATP-7A, ATP-7B), whereas bioinformatics analysis shows no consensus sequence for cluster formation.

Dicopper thiolate clusters are found in dimeric proteins at the protein−protein contact interface as in CopZ, Cox11, and Ccs. Bacterial copper chaperone CopZ contains two conserved Cys residues and forms dimers with a dinuclear copper thiolate cluster at the protein−protein contact interface.[13] A similar dinuclear Cu_2S_4-type cluster located at the dimeric interface exists in copper chaperone Cox11, monomers of which contain a CFCF metal-binding motif.[14,15] The dicopper thiolate cluster has also been suggested to exist in dimeric Ccs.[16]

Polycopper thiolate clusters are involved in transport and storage of Cu(I) ions. Mechanisms of their biological functioning are largely unknown. Only a few proteins containing polycopper thiolate clusters have been structurally characterized. In part, this may be related to complicated preparative work with Cu(I) proteins, but the conformational dynamics and structural heterogeneity of these proteins cause additional complications. A high-resolution structure is known only for yeast metallothionein Cup1, which contains 61 amino acid residues including 12 Cys.[17] The X-ray structure of CuCup1 displays a octacopperdecathiolate (Cu_8S_{10})-type cluster.[12] Structural information for other clusters is derived mainly from EXAFS studies, which cannot provide atomic coordinates but can reveal a number of fundamental structural parameters like metal to ligand stoichiometry as well as metal to ligand and metal to metal distances in the clusters.

Energetic and kinetic principles of polycopper thiolate cluster formation are poorly understood. Many in vitro experiments demonstrate that copper thiolate clusters are formed cooperatively;[4,18] however, the driving force and mechanisms of cluster formation are unknown. As a variety of different proteins form similar copper thiolate clusters, we might suggest that sequence plays a secondary role in cluster formation, which seems to be determined by the availability of multiple thiolates in the protein.

* To whom correspondence should be addressed. E-mail: tamm@yki.ttu.ee. Fax: +372-6202020.

10.1021/jp8114644 CCC: $40.75
Published on Web 07/16/2009

It is reasonable to assume that copper thiolate cluster formation might be determined by purely energetic factors, which are, however, unknown. Energetic aspects of cluster formation could be studied by quantum chemical approaches. However, their application to proteins is limited as the structures of proteins containing polycopper thiolate clusters are unknown.

One possibility to get information about energetic and structural aspects of biological copper thiolate clusters is the introduction of simple (bio)inorganic model systems. Low-molecular analogues for polycopper thiolate clusters are well-known in bioinorganic chemistry and many basic low-molecular polycopper thiolate clusters have been structurally characterized.[19−22] These structures serve as good models for biological polycopper thiolate clusters. In combination with quantum chemical approaches, they may reveal energetic parameters of the formation and stability of biologically relevant polycopper thiolate clusters.

Until now, computations have been performed for some copper−ligand complexes and for a limited number of copper thiolate clusters. There has been a number of computational surveys about the nature of various copper−ligand complexes, including complexes with biologically relevant ligands. In a recent study, interactions of Cu(I)/Cu(II) ions with sulfur-, oxygen-, and nitrogen-containing ligands were investigated.[23] The results indicated that the complexes formed with nitrogen-containing ligands have the highest stabilization energy, followed by the sulfur- and finally oxygen-containing ligands. However, the authors point out that this preference must be taken with care since the remaining part of the ligated molecule can substantially mask electron density characteristics. The three- and four-coordinated structures are favored in the case of the H_2S molecule occupying the first solvation shell of Cu(I).[23]

So far, computational studies have been focused mainly on copper thiolate clusters relevant for material science. Biologically relevant copper thiolate clusters have not been studied by the quantum chemical approach; however, such studies would allow us to get unique information about energetic and structural aspects of biological copper thiolate clusters and unravel basic principles for their formation and biological functioning.

In this study, we used density functional theory (DFT) simulations for the investigation of the structure and stability of a systematic series of Cu_xS_y-type clusters. The effects of the cluster composition on the energetics of cluster formation and cluster structure demonstrated a favorable energetic effect of cluster formation and revealed basic principles for the formation of different biologically relevant polycopper thiolate clusters. Moreover, the influence of slight structural perturbations and the charges of clusters on the energetics of copper thiolate clusters is also analyzed and discussed.

Computational Methods

Density functional theory calculations were performed with the BP86 functional and the TZVPP basis set. For an additional gain in speed, the resolution of identity (RI) approximation was used. Geometries were fully optimized without imposing symmetry constraints. Where the possibility of the formation of several conformers was envisaged, several alternative structures were prepared. For the larger structures, up to six minima on the potential energy surface were identified. Only the results for those with the lowest energy are presented. Also, the stability of possible high-spin (two or four unpaired electrons) configurations was tested. For some of these, convergence of SCF was not achieved, while for the rest, the energies of the triplet and quintuplet states were found to be higher than that for the singlet state. We conclude that the systems studied here have singlet ground states.

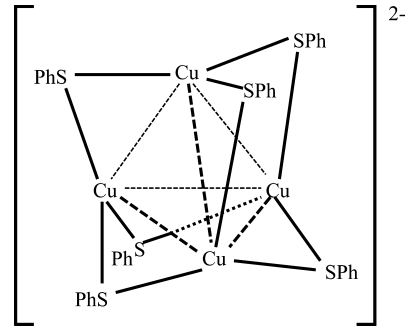

Figure 1. Structure of the copper thiolate cluster $[Cu_4(SPh)_6]^{2-}$.

Vibrational analysis of the obtained stationary points was performed in order to confirm the lack of imaginary vibrational frequencies and to calculate the zero-point vibrational energy. Thermal contributions to the enthalpy were estimated based on the vibrational energies. The enthalpies and Gibbs free energies of the systems were calculated for 298 K. The energies used in the tables and discussions in this work are the ΔE, ΔH, and ΔG values including zero-point and thermal corrections.

Solvent effects were estimated with the Cosmo model,[24] using the values of the dielectric permittivity for water ($\varepsilon = 78.5$) and an "average" protein ($\varepsilon = 8$). Geometries were reoptimized and vibrational analysis was repeated for the solvated systems. However, since the vibrational entropy-related terms of the free energy are already included in the Cosmo model, the gas-phase zero-point energies and corresponding thermal corrections were used in calculations of the ΔH and ΔG values. Correspondingly, only gas-phase entropies are listed in the tables.

All calculations were performed with the Turbomole versions 5.6 and 5.10 software.[25,26] The final results reported here have all been obtained with version 5.10.

Model Geometries

We constructed a selection of $[Cu_x(SMe)_y]^{n-}$ geometries ($x \leq 5$, $y \leq 6$) based on low-molecular crystal structures for $[Cu_2(SMe)_4]^{2-}$, $[Cu_4(SMe)_6]^{2-}$, and $[Cu_5(SMe)_6]^{-}$ clusters[21,27] by adding or removing Cu^+/SMe^- units.

These clusters are similar to the well-known $[Cu_4(SPh)_6]^{2-}$ clusters[28,29] shown in Figure 1.

In the following text, we use the abbreviations Cu_xS_y to indicate the number of Cu and S atoms in the cluster. The presence of methyl or other organic substituents bound to each sulfur atom is implied. Also, the charge, even if different from zero, is not included in these abbreviations. We also use the term "energy of formation" in the loose sense of the ΔE or ΔH of the reaction, leading to the formation of species being discussed out of simpler compounds, as outlined below. These energies of formation should not be confused with the enthalpies of formation as defined in standard thermodynamics. None of the latter are estimated in this study.

Results and Discussion

Calculations of $[Cu_x(SMe)_y]^{n-}$ Cluster Formation. Calculated energetic parameters of cluster formation depend substantially on the nature of the initial Cu(I) complex representing "free" copper. In order to get reasonable estimates, this complex should model the biological situation as much as possible. To avoid disproportionation and oxidation, Cu(I) ions in biological systems are often bound to the ubiquitous antioxidant molecule

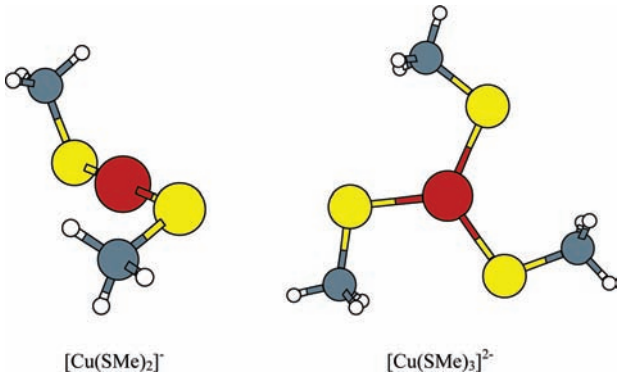

Figure 2. Gas-phase structures of the bicoordinated and tricoordiated small clusters, optimized at the BP86/TZVPP level.

glutathione (GSH), the cellular concentration of which is in the millimolar range. The coordination of copper thiolate complexes is normally trigonal planar; however, linearly coordinated examples are also known.

Therefore, we started our cluster calculations from trigonal $[Cu(SMe)_3]^{2-}$ and linear $[Cu(SMe)_2]^-$ complexes (Figure 2) that model Cu(I) bound to GSH or other low-molecular thiol reagents. For the sake of comparability of the energetic effects of formation of different $Cu(I)_xS_4$ and $Cu(I)_xS_6$ clusters, all reactions were set up in such a way that the count of Cu−S bonds was equal on both sides of the reaction. The requirement of the preservation of the number of Cu−S bonds leads to the unique definition of the cluster-formation reactions, listed as A1···C4 below.

Energetic Parameters of Cluster Formation. Results of density functional calculations for different polycopper thiolate clusters are presented in Tables 1 and 2 and illustrated in Figure 3. For most of the $Cu(I)_xS_4$ and $Cu(I)_xS_6$ clusters, ΔE in the gas phase is negative, which indicates that the system goes through a rearrangement of Cu−S bonds into a lower energetic state relative to that of the mononuclear linearly and trigonally coordinated Cu(I) unit structures.

Solvation has substantial influence on the energetic parameters, which depend on the ionic charge of the clusters and differences between the numbers of species on the two sides of the reaction. Generally, the solvation-caused increase in the ΔE and ΔG values was higher for solvents with higher polarity of the solvent, and in some cases, the ΔE and ΔG values became even positive in the solvent. The absolute values of energy differences, however, became smaller as the ε of the solvent increased. This is reflected in the different energy scales used in Figure 3.

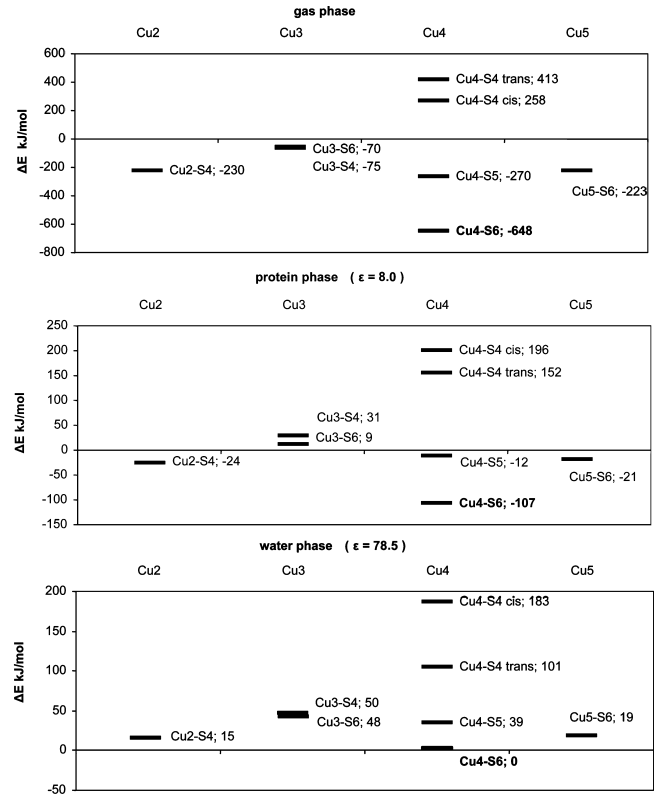

Figure 3. Overall comparison of ΔE of cluster formation (Tables 1 and 2) in three different phases (gas, $\varepsilon = 8$, and $\varepsilon = 78.5$).

Redistribution of charge among the species is obviously associated with very large energetic effects since the dependence of solute−solvent interactions on the charge number is approximately quadratic. An increase in the number of species in all forward reactions also leads to a large positive ΔS value. Due to this, ΔG is always lower than ΔE. However, both parameters can be used for characterization of the energetics of cluster formation. Reactions can be compared to each other on the basis of ΔG values only if $\Delta n_{species}$ are equal for these reactions. Here, $\Delta n_{species} = \Sigma n_p - \Sigma n_r$, where n_p and n_r are number of species of products and reactants, respectively.

Tetrathiolate Clusters. The following formation reactions, preserving the total number of Cu−S bonds, were assumed in the reaction energy calculations

TABLE 1: Energies of Formation of Cu_nS_4 Clusters

			ΔE, kJ/mol			ΔH, kJ/mol			ΔG, kJ/mol			ΔS, J/mol/K
reaction	num of Cu−S bonds	$\Delta n_{species}$	gas	$\varepsilon = 8$	$\varepsilon = 78.5$	gas	$\varepsilon = 8$	$\varepsilon = 78.5$	gas	$\varepsilon = 8$	$\varepsilon = 78.5$	gas
A1	6	1	−230	−24	15	−234	−28	12	−264	−58	−19	101
A2	7	1	−75	31	50	−80	26	45	−91	15	34	37
A3	8	1	413	152	101	404	144	93	390	130	79	46
A4	9	2	258	196	183	246	183	171	198	135	123	161

TABLE 2: Energies of Formation of Cu_nS_6 Clusters

			ΔE, kJ/mol			ΔH, kJ/mol			ΔG, kJ/mol			ΔS, J/mol/K
reaction	num of Cu−S bonds	$\Delta n_{species}$	gas	$\varepsilon = 8$	$\varepsilon = 78.5$	gas	$\varepsilon = 8$	$\varepsilon = 78.5$	gas	$\varepsilon = 8$	$\varepsilon = 78.5$	gas
B1	9	1	−70	9	48	−75	5	20	−91	−12	3	55
B2	12	3	−648	−107	0	−660	−119	−12	−734	−192	−85	247
B3	12	2	−223	−21	19	−234	−31	9	−270	−67	−27	121
B4	10	2	−270	−12	39	−279	−21	29	−321	−63	−12	140

$$2[Cu(SMe)_3]^{2-} \rightarrow [Cu_2(SMe)_4]^{2-} + 2SMe^- \quad (A1)$$

$$2[Cu(SMe)_2]^- + [Cu(SMe)_3]^{2-} \rightarrow [Cu_3(SMe)_4]^- + 3SMe^- \quad (A2)$$

$$4[Cu(SMe)_2]^- \rightarrow \textit{trans}\text{-}Cu_4(SMe)_4 + 4SMe^- \quad (A3)$$

$$3[Cu(SMe)_2]^- + [Cu(SMe)_3]^{2-} \rightarrow \textit{cis}\text{-}Cu_4(SMe)_4 + 5SMe^- \quad (A4)$$

[Cu$_2$(SMe)$_4$]$^{2-}$. In the set of Cu(I)$_x$S$_4$ clusters (Figure 4), the biologically relevant $[Cu_2(SMe)_4]^{2-}$ cluster stands out as the most stable structure. Distinct from all other clusters, its ΔG value in the solvent field is negative. The $[Cu_2(SMe)_4]^{2-}$ cluster has two terminal and two bridging thiolate groups. Both copper ions are in trigonal planar coordination, whereas the angle between the corresponding planes is 117°. Terminal Cu−S distances are 2.23 Å, bridging Cu−S distances are close to 2.4 Å, and the Cu−Cu distance is 2.69 Å.

[Cu$_3$(SMe)$_4$]$^-$. The next most stable structure is the $[Cu_3(SMe)_4]^-$ cluster, which might be formed in a nonpolar environment. Formation of the $[Cu_3(SMe)_4]^-$ cluster is entropically comparable to similar reactions for $[Cu_2(SMe)_4]^{2-}$ and *trans*-$[Cu_4(SMe)_4]$ ($\Delta n_{species} = 1$). Thus, in terms of ΔG at $\varepsilon = 8$, $[Cu_3(SMe)_4]^-$ formation lies at the borderline of spontaneity but still has a ∼70 kJ/mol higher value than the corresponding ΔG for the $[Cu_2(SMe)_4]^{2-}$ cluster.

The $[Cu_3(SMe)_4]^-$ cluster has one terminal and three bridging thiolates. Two copper ions are bent bicoordinated, and one copper is tricoordinated (Figure 4). The cluster possesses a ring structure which also occurs elsewhere, for example, in the known neutral trinuclear framework of $[Ag(SC(SiPhMe_2)_3]_3$,[30] where tricoordinated metal is out of the plane and coordinated to a terminal sulfur. The S−Cu−S angles at bicoordinated coppers are slightly off from linear at 165° and 167°. Angles at tricoordinated Cu atoms are distorted by 20° due to repulsion between methyl groups. Corresponding Cu−S bond lengths are also longer than usual (approaching 2.4 Å). The methyl group at the tricoordinated copper is twisted sideways. Another minimum of equal energy exists where the group is bent in the opposite direction, the structure being a mirror image of the one shown in Figure 4.

[Cu$_4$(SMe)$_4$]. The other possible tetrathiolate clusters are two neutral isomers of $[Cu_4(SMe)_4]$. These clusters with similar stoichiometry are geometrically rather different. The cis form has a cage-like structure, with nine Cu−S bonds, having a tetravalent sulfur at one apex and trivalent copper at the opposite end (bottom in Figure 4). Three coppers are bicoordinated, and one is tricoordinated. The metal ions are located near apexes of an imaginary tetrahedron, while the sulfurs form another spatially reversed tetrahedron. This geometry appears to be somewhat strained as the bond angles of the four-coordinated sulfur are distorted from the usual tetrahedral form (C−S−Cu angles of ∼135°).

The *trans*-$[Cu_4(SMe)_4]$ (eight Cu−S bonds) cluster has all four copper atoms in a nearly linear configuration, while the metal atoms are at the corners of a square-like structure (Figure 4). The ring is not planar, however, with the sulfurs having 75° bond angles. This tetrameric ring structure with D_{2d} symmetry minimizes strain in linear metal coordination and angular coordination at sulfur.

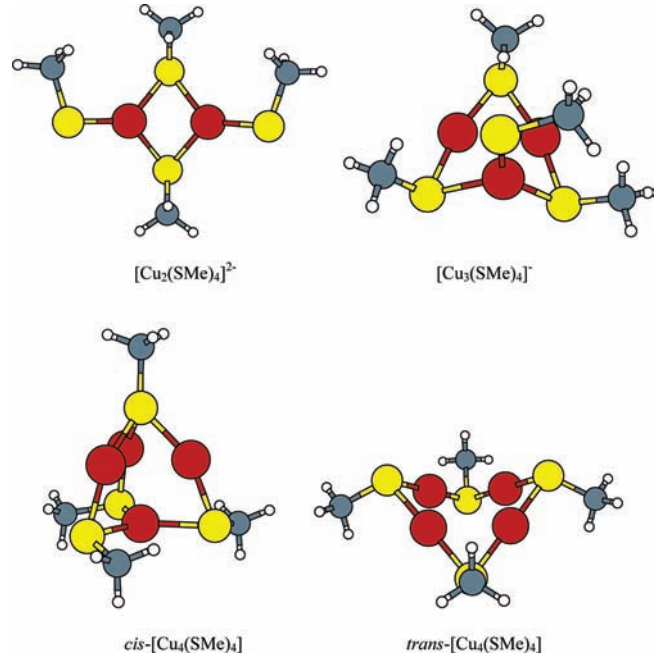

Figure 4. Gas-phase structures of Cu(I)$_x$−S$_4$ clusters optimized at the BP86/TZVPP level.

The formation of both isomers is energetically strongly unfavorable already in the gas phase. At the same time, in terms of the absolute energies, the trans form is more stable than the cis isomer by 155 kJ/mol in the gas phase and by 82 kJ/mol in water. The positive energy change in the formation reaction of the cis form may be related to solvent effects (one 2− charge is replaced by two 1− charges). The unfavorable energy of formation of the trans form of the $[Cu_4(SMe)_4]$ cluster is in slight disagreement with experimental evidence of the existence of similar clusters containing Cu, Ag, and Au.[30] The presence of an increasing number of the small-radius SMe^- ions on the right-hand side of our postulated reactions of formation may also cause an apparent increase of reaction energies in the A1−A4 series.

Penta- and Hexathiolate Clusters. The reactions involving five or six sulfur atoms have varying changes in species count ($\Delta n_{species}$), and therefore, the changes in entropy are not directly comparable between them. However, the relative stabilities of clusters could be obtained by comparing either ΔE or ΔH values.

The following reactions of formation were considered

$$3[Cu(SMe)_3]^{2-} \rightarrow [Cu_3(SMe)_6]^{3-} + 3SMe^- \quad (B1)$$

$$4[Cu(SMe)_3]^{2-} \rightarrow [Cu_4(SMe)_6]^{2-} + 6SMe^- \quad (B2)$$

$$3[Cu(SMe)_2]^- + 2[Cu(SMe)_3]^{2-} \rightarrow [Cu_5(SMe)_6]^- + 6SMe^- \quad (B3)$$

$$2[Cu(SMe)_2]^- + 2[Cu(SMe)_3]^{2-} \rightarrow [Cu_4(SMe)_5]^- + 5SMe^- \quad (B4)$$

All of the reactions of formation are favorable in the gas phase. However, in the water phase, the only favorable reaction is the formation of the $[Cu_4(SMe)_6]^{2-}$ structure (Figure 3).

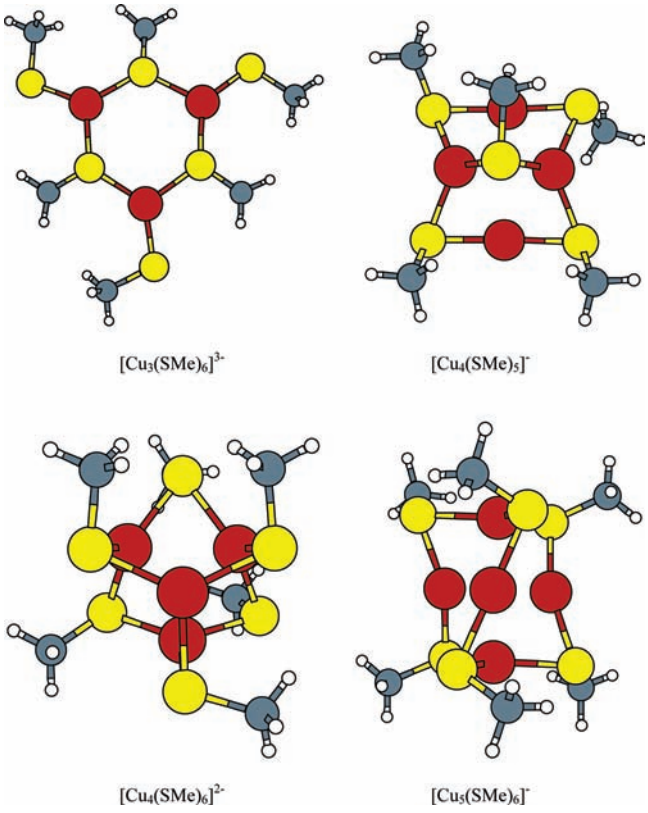

Figure 5. Gas-phase structures of $Cu(I)_x-S_6$ clusters optimized at the BP86/TZVPP level.

[Cu4(SMe)6]2−. Among the hexathiolate clusters (Figure 5), $[Cu_4(SMe)_6]^{2-}$ stands out as the most stable structure characterized by all-bridging thiolates and all-tricoordinated Cu(I) atoms. The geometry of the Cu_4S_6 cluster resembles an adamantane-like polyhedron with four coppers at the tips of a larger imaginary tetrahedron, the edges of which are bridged by sulfur atoms. Many mutual orientations of the methyl groups are possible. We did not find the more regular ones to yield lower energies, while the energy differences between conformations were minor. All of the Cu(I) ions are tricoordinated (Figure 5). $[Cu_4(SMe)_6]^{2-}$ has the same number of Cu−S bonds (12) as the $[Cu_5(SMe)_6]^-$ framework, but the latter has three Cu(I) atoms in a linear arrangement. The energetic difference between the linear and trigonal configurations can be seen as the large differences in the gas-phase ΔE values of the formation reactions of corresponding structures (reactions B2 and B3), both of which involve an equal number of Cu−S bonds. Formation of $[Cu_4(SMe)_6]^{2-}$ (reaction B2) is characterized by a large positive ΔS value originating from the largest change in the number of species ($\Delta n_{species} = 3$).

[Cu5(SMe)6]−. According to our calculations, the next most stable structure after the Cu_4S_6 one is the $[Cu_5(SMe)_6]^-$. In terms of ΔE, the $[Cu_5(SMe)_6]^-$ cluster is ∼19 kJ/mol less stable in the water phase than $[Cu_4(SMe)_6]^{2-}$. The latter result is in agreement with the cooperative nature of the formation of tetracopper thiolate clusters in mass spectrometric measurements of Ctr1[4] and Cox17,[18] where at higher metal−protein stoichometries, Cu_5S_6 is also observed. The metal ions form a trigonal bipyramid, which is incorporated into a {S6} trigonal prism, thus allowing this framework to be sterically more flexible. The trigonal {S6} prism can be twisted around the central vertical axis up to the limit of the trigonal antiprism (Figure 5).

[Cu4(SMe)5]−. In the monoanionic pentathiolate $[Cu_4(SMe)_5]^-$, two copper atoms have distorted linear configuration (175°), whereas the two remaining ones have trigonal coordination connected via a common sulfur bridge. The geometry of the $[Cu_4(SMe)_5]^-$ cluster resembles the one of all-tricoordinated $[Cu_4(SMe)_6]^{2-}$ and is therefore discussed here. The latter contains only one additional (sixth) sulfur bridge, which bends two Cu atoms from their nearly linear configuration into a trigonal one (Figure 5). In terms of the energies of formation, the $[Cu_4(SMe)_5]^-$ (reaction B4) cluster is comparable to $[Cu_5(SMe)_6]^-$ (reaction B3). In the gas phase, the formation of $[Cu_4(SMe)_5]^-$ is more favorable than that of $[Cu_5(SMe)_6]^-$. On the other hand, the solvent effects of the latter reaction are more pronounced; therefore, the formation of $[Cu_5(SMe)_6]^-$ in solution is more favorable. The solvation energy E_{solv}(78.5) for $[Cu_5(SMe)_6]^-$ is 5 kJ/mol larger than that for $[Cu_4(SMe)_5]^-$.

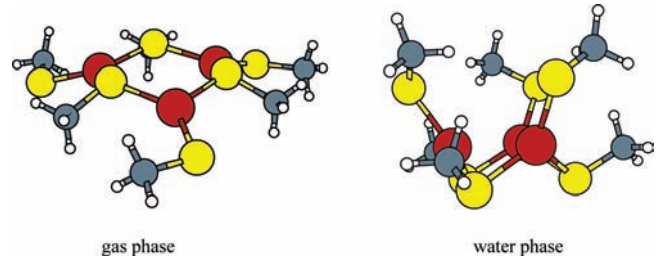

Figure 6. Gas-phase and water-phase structures of the $[Cu_3(SMe)_6]^{3-}$ cluster.

[Cu3(SMe)6]3−. In the $[Cu_3(SMe)_6]^{3-}$ cluster, all Cu(I) ions are tricoordinated and linked together via bridging sulfurs into a $\{Cu_3S_3\}$ ring in the chair conformation. The remaining three terminal thiolates are arranged in a way that provides a vacant metal position for a fourth copper atom with trigonal coordination. This position is filled in $[Cu_4(SMe)_6]^{2-}$ (Figure 5). Calculated energy changes for the reaction

$$[Cu_3(SMe)_6]^{3-} + [Cu(SMe)_3]^{2-} \rightarrow [Cu_4(SMe)_6]^{2-} + 3SMe^-$$

are $\Delta E_{gas} = -578$ kJ/mol, $\Delta E_8 = -116$ kJ/mol, and $\Delta E_{78.5} = -25$ kJ/mol, which demonstrates that such metal incorporation is energetically favored, more so in the gas phase. Another important factor for the stabilization of the tetranuclear unit compared to the trinuclear one is the lower negative charge of the latter due to incorporation of the fourth copper atom.

The gas-phase optimized geometry of the structure differs significantly from its solvent field geometry (Figures 5 and 6). In the solvent field, the terminal thiolates retain their compact metal-bound positions similar to those in the $[Cu_4(SMe)_6]^{2-}$ structure, even though the fourth metal atom is removed. In the gas phase, the terminal thiolates repel each other, and the geometry flattens. This emphasizes the possible vital role of electrostatic interactions between the environment and the cluster on the pathway of $[Cu_4(SMe)_6]^{2-}$ formation.

Charge of Clusters. Most polycopper thiolate clusters studied here are anionic, and therefore, their charge has to be stabilized in the proteins. For instance, in most zinc-containing structures found in the PDB database, the Zn^{2+} coordination sphere is surrounded by polar and charged groups, giving rise to a heterogeneous dielectric environment. The average protein potential on the $ZnCys_3His$ coordination sphere was calculated to be +14 kcal/mol/e.[31] This is a substantial effect given the values of the energies of formation calculated in this work in the homogeneous solvent field.

TABLE 3: Energies of Solvation from the Gas Phase ($\varepsilon = 1$) to the Water Phase ($\varepsilon = 78.5$)

structure	charge of the cluster	ΔE_{solv}, kJ/mol
$[Cu_3(SMe)_6]^{3-}$	−3	−1323
$[Cu(SMe)_3]^{2-}$	−2	−774
$[Cu_2(SMe)_4]^{2-}$	−2	−700
$[Cu_4(SMe)_6]^{2-}$	−2	−639
$[Cu(SMe)_2]^{-}$	−1	−230
$[Cu_3(SMe)_4]^{-}$	−1	−204
$[Cu_4(SMe)_5]^{-}$	−1	−192
$[Cu_5(SMe)_6]^{-}$	−1	−187
$Cu(HSMe)_2SMe$	0	−61
$Cu_2(SMe)_2(HSMe)_2$	0	−54
cis-$Cu_4(SMe)_4$	0	−33
trans-$Cu_4(SMe)_4$	0	−26
$[Cu(HSMe)_3]^{+}$	1	−195

Calculated solvation energies for the gas to water transition of the studied complexes are presented in Table 3. As can be seen from this data, the component of the electrostatic potential makes up the most substantial amount of the solvation energy (ΔE_{solv}) compared to other factors. As expected, the solvation effect is approximately proportional to the square of the charge of the system. For example, the solvation energy (from the gas to water phase) of $[Cu_3(SMe)_6]^{3-}$ (charge 3−) is ∼−1300 kJ/mol, whereas for $[Cu_4(SMe)_6]^{2-}$ (charge 2−), it is ∼−640 kJ/mol. ΔE_{solv} for the neutral mononuclear $Cu(HSMe)_2SMe$ (−61 kJ/mol) is similar to that of the neutral tetranuclear $[Cu_4(SMe)_4]$ isomers (−33 and −26 kJ/mol, respectively). Therefore, the dependence of the energies of formation on the charge of the species could be studied on the example of the simplest cluster, $[Cu_2(SMe)_4]^{2-}$, which has two terminal thiolates that can be readily protonated. This changes the charge of the species with little effect on the geometry and the volume of the molecule.

Protonation of the $[Cu_2(SMe)_4]^{2-}$ Cluster. The $[Cu_2(SMe)_4]^{2-}$ structure is usually observed as a complex at the interface of protein units. Obviously, it is prone to protonation as it is dianionic and more exposed to aqueous solvent. Geometries with protonated thiolates were optimized at the same level of theory as that reported above. The resulting structures were compared in terms of Cu−S bond lengths and cluster formation energetics in their gas phase as well as in the water solvent field. A characteristic feature of the $[Cu_2(SMe)_4]^{2-}$ cluster is the trigonal complexing of copper atoms by thiolates, two of which are bridging and two of which are terminal (Figure 4). Protonation of any of the two sulfur bridges results in dissociation of the bridge and gives rise to a set of isomers. Surprisingly, this happens even when the nearby terminal thiolate is protonated. In fact, the only isomer that remains intact is the doubly protonated $Cu_2(SMe)_2(HSMe)_2$ structure where both terminal thiolates are protonated. The all-protonated $[Cu_2(HSMe)_4]^{2+}$ decomposes as well. Similar observations were made for the Cu_4S_6-type clusters, where all thiolates are bridging and the Cu−S bond breaks after protonation of any of the thiolates.

Protonation of biological polycopper thiolate clusters might be one possibility for their destruction and metal release, which might occur by the influence of pH fluctuations caused by cellular metabolism or signaling and upon protein transport into cellular compartments exhibiting lower pH values (lysosomes, mitochondrial intermembrane space, etc). In the following sections, the effects of protonation on the energies of formation and Cu−S bond length of the $Cu_2(SMe)_2(HSMe)_2$ are discussed.

Energies of Formation of the $Cu_2(SMe)_2(HSMe)_2$ Cluster. The following reactions leading to the formation of the $Cu_2(SMe)_2(HSMe)_2$ cluster from different constituents were considered. The corresponding energetic data are presented in Table 4.

$$2[Cu(SMe)_3]^{2-} \rightarrow [Cu_2(SMe)_4]^{2-} + 2SMe^{-} \quad (C1)$$

$$Cu(HSMe)_2SMe + [Cu(SMe)_3]^{2-} \rightarrow Cu_2(SMe)_2(HSMe)_2 + 2SMe^{-} \quad (C2)$$

$$2Cu(HSMe)_2SMe \rightarrow Cu_2(SMe)_2(HSMe)_2 + 2HSMe \quad (C3)$$

$$[Cu(HSMe)_3]^{+} + [Cu(SMe)_3]^{2-} \rightarrow Cu_2(SMe)_2(HSMe)_2 + HSMe + SMe^{-} \quad (C4)$$

Calculated gas-phase energies of formation of the neutral $Cu_2(SMe)_2(HSMe)_2$ cluster indicate that in this doubly protonated state, the formation of such a cluster is relatively less favored than that in the dianionic case (reactions B1 and C1). This is related to the higher stabilization of the neutral mononuclear $Cu(HSMe)_2SMe$ complex when compared to that of $Cu_2(SMe)_2(HSMe)_2$.

In a reaction where all species are electroneutral due to protonation (reaction C3), the feasibility of cluster formation is further reduced. Furthermore, the ΔE values in the gas phase and in the water phase become quite close, the water phase value becoming even negative. The ΔE value corresponding to the protein environment is expected to be in between the corresponding gas and water phase values. It can be concluded that in real systems where charges are neutralized by the environment, phase transitions between the protein environment and water environment involve small energy differences since small solvation energies are involved. In contrast, the very large gas-phase ΔE value for reaction C4 involving triply protonated $[Cu(HSMe)_3]^{+}$ species results from the fact that the gas-phase proton affinity of SMe^{-} is ∼500 kJ/mol greater than that of neutral $Cu(HSMe)_2SMe$.

Comparison of Cu−S Bond Lengths in Protontaned and Nonprotonated $[Cu_x(SMe)_y]^{n-}$ Clusters. The average Cu−S bond lengths of some representative clusters are listed in Table 5. In $[Cu_2(SMe)_4]^{2-}$, the bridging Cu−S bond is shorter than that for the terminal Cu−S bond by 0.13 Å. The difference is 0.08 Å for the single stable protonated cluster, $Cu_2(SMe)_2$-

TABLE 4: Energies of Formation of $Cu_2(SMe)_2(HSMe)_2$ Clusters

		ΔE, kJ/mol		ΔH, kJ/mol		ΔG, kJ/mol		ΔS, J/mol/K
reaction	$\Delta n_{species}$	gas	$\varepsilon = 78.5$	gas	$\varepsilon = 78.5$	gas	$\varepsilon = 78.5$	gas
C1	1	−230	15	−234	12	−264	−19	101
C2	1	−141	37	−145	33	−170	8	81
C3	1	−69	−28	−74	−32	−102	−61	95
C4	1	−639	−40	−642	−43	−670	−71	94

TABLE 5: Comparison of Average Cu−S Bond Lengths (Å) in Cu_2−Thiol/Thiolate Complexes

	$[Cu_2(SMe)_4]^{2-}$		$Cu_2(SMe)_2(HSMe)_2$	
Cu−S	gas	$\varepsilon = 78.5$	gas	$\varepsilon = 78.5$
bridging	2.36	2.34	2.30	2.31
terminal	2.23	2.21	2.22	2.23
Δ^a	0.13	0.13	0.08	0.08

[a] Δ denotes the difference of the Cu−S bridging and terminal bond lengths.

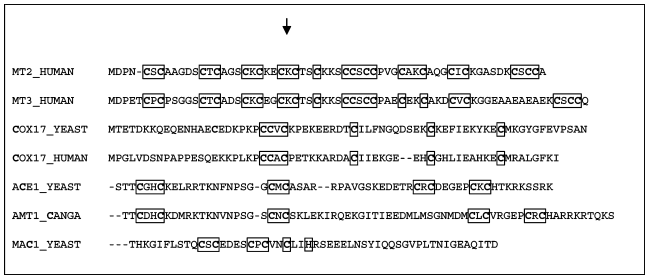

Figure 7. Comparison of protein sequences forming Cu(I)−S_y clusters. Arrows show the position of the Cys residue used as the alignment point in CLUSTALW.

$(HSMe)_2$. The corresponding bond distances in vacuo and in the water phase differ only by 0.01−0.02 Å. The metal−S bond length has been proposed as a geometric criterion for the protonation state of cysteine in Zn-thiol/thiolate and Cd-thiol/thiolate complexes in proteins.[32] The Zn/Cd−Cys bond is notably longer in protonated complexes than that in the nonprotonated ones. However, for Cu(I)-thiol/thiolate systems, the effect of protonation is insignificant; the difference between terminal and bridging Cu−S−/SH bond lengths is reduced by only 0.05 Å. Also, in the simple unit structures such as the CuS_3, protonation has very little influence on the Cu−S distances. Nevertheless, HSMe dissociates from the singly protonated $[Cu(SMe)_2(HSMe)]^{2-}$ complex, leading to an "infinite" bond length.

On the other hand, the Cu−S bond length depends on the Cu^+ configuration. For example, the divalent Cu in $Cu(SMe)_2^-$ has 2.17 Å Cu−S bonds, while in the trivalent configuration, such as $Cu(SMe)_3^{2-}$, the bond length is 2.31 Å. For the clusters $[Cu_4(SMe)_6]^{2-}$ and $[Cu_5(SMe)_6]^-$, linear and trigonal Cu−S distances are 2.22 and 2.30−2.33 Å, respectively, slightly longer than those for corresponding simple unit structures.

Our conclusion is that the protonation state of the terminal sulfur in clusters such as those of the type Cu_2S_4 cannot be inferred from the Cu−S bond distances because natural clusters in proteins could be deformed and differences of distances in the range of 0.1 Å are experimentally not well distinguished.

Biological Implications of the Energetics of Cluster Formation. On the basis of the energies of the formation of the model clusters from the simple unit structures (types CuS_2 and CuS_3), the Cu_4S_6-type geometry is the most stable structure as compared to all other possible Cu(I)−S cluster structures considered here (Figure 3). This conclusion can be made in the case of all modeled phases, whereas the gas-phase energies of formation (ΔE) are relatively large and inclusion of the solvation effects via the Cosmo model reduces the energetic effects of cluster formation. Relative stabilities of the clusters are also similar in different phases, with exception of the monoanionic $[Cu_4(SMe)_5]^-$ and $[Cu_5(SMe)_6]^-$. Monoanionic complexes are more favored in polar solvents due to the increasing of the solvation energy of charged clusters. In proteins, the polycopper thiolate clusters are solvent-shielded,[33] however, as they are surrounded and stabilized by a polar polypeptide backbone and by hydrophilic residues located on the protein surface,[12] which might contribute to the stabilization of charged clusters.

Cooperativity of Cu_4S_6-Type Cluster Formation. The present work mapped clusters with different Cu/thiolate stoichiometries that might exist as intermediate forms in the pathway of the formation of Cu_4S_6-type clusters in nature. Our calculations demonstrate large energy differences between the $[Cu_4(SMe)_6]^{2-}$ and other structures, which provides an energetic background for cooperative formation of the Cu_4S_6-type cluster observed in a number of in vitro experiments. The calculations support the view that cluster formation starts from mono- or dinuclear complexes, which have an excess of coordination capacity for the binding of additional metal ions. Such a situation is evident also in the case of the $[Cu_3(SMe)_6]^{3-}$ cluster (Figure 4), where the large energetic effect of metal incorporation into the $[Cu_3(SMe)_6]^{3-}$ makes the formation of $[Cu_4(SMe)_6]^{2-}$ fast and cooperative.

Functional Role of Cu_4S_6-Type Clusters. Polycopper thiolate clusters are formed in a variety of proteins from different functional classes, including copper transporters, copper chaperones, transcriptional activators, copper storage proteins, metallothioneins, and others. Comparison of protein sequences, which have experimentally been shown to form Cu_4S_6-type structures (Ace1, Amt1, Mac1, Cox17), clusters, and higher-order clusters (MTs) (Figure 7) indicates that, besides short CXC and CXXC motifs, there are no evolutionally conserved motifs or Cys positions in the cluster-forming fragments of these proteins. Therefore, it is reasonable to suggest that the formation of polycopper thiolate clusters is not dictated by a specific sequence but by the presence of multiple Cys residues. These structures might play a rather general role connected, for instance, with sequestration of excessive Cu(I) ions from the cellular environment.

Conclusions

In this work, a density functional theory modeling of the series of $[Cu_x(SMe)_y]^{n-}$-type copper thiolate clusters was performed. The effect of protonation on the energies of formation was studied in the case of the $[Cu_2(SMe)_4]^{2-}$ cluster. All calculations were performed in three different environments, including the gas phase ($\varepsilon = 0$), protein interior ($\varepsilon = 8$), and water ($\varepsilon = 78.5$) solution, with the use of a continuum model. The energetic effects of the formation of the clusters from simple copper−sulfur compounds were estimated. The results were compared with experimentally known aspects of copper thiolate cluster composition and chemistry in different copper-containing proteins.

In light of the results of the calculations and considering the absence of common sequential motifs, the formation of polycopper thiolate clusters should be guided primarily by the energy of the cluster formation. The sequence of the Cys-rich region in the protein plays a secondary role. Thus, it is reasonable to suggest that copper thiolate clusters are not functional units in the proteins but might rather play the primary role in sequestration of excessive copper ions from the environment. Following this line of reasoning, we suggest that the formation of polycopper thiolate clusters might lock different proteins into conformations that bind a high stoichiometry of copper ions and protect these from interaction with oxygen derivatives. In some cases, copper thiolate clusters might also be used for copper sensing and gene regulation, like in the case of yeast transcription factor Mac1.

Acknowledgment. This work was supported by Estonian Science Foundation Grant 7191.

References and Notes

(1) Brown, K. R.; Keller, G. L.; Pickering, I. J.; Harris, H. H.; George, G. N.; Winge, D. R. *Biochemistry* **2002**, *41*, 6469.
(2) Palumaa, P.; Kangur, L.; Voronova, A.; Sillard, R. *Biochem. J.* **2004**, *382*, 307.
(3) Eisses, J. F.; Stasser, J. P.; Ralle, M.; Kaplan, J. H.; Blackburn, N. J. *Biochemistry* **2000**, *39*, 7337.
(4) Xiao, Z.; Loughlin, F.; George, G. N.; Howlett, G. J.; Wedd, A. G. *J. Am. Chem. Soc.* **2004**, *126*, 3081.
(5) Cobine, P. A. *Biochemistry* **2000**, *39*, 6857.
(6) Ralle, M. *J. Inorg. Biochem.* **2004**, *98*, 765.
(7) Kägi, J. H. R.; Schäffer, A. *Biochemistry* **1988**, *27*, 8509.
(8) Chen, P.; Munoz, A.; Nettesheim, D.; Shaw, C. F.; Petering, D. H. *Biochem. J.* **1996**, *317*, 395.
(9) Jensen, L. T.; Peltier, J. M.; Winge, D. R. *J. Biol. Inorg. Chem.* **1998**, *3*, 627.
(10) Roschitzki, B.; Vasak, M. *J. Biol. Inorg. Chem.* **2002**, *7*, 611.
(11) Pountney, D.; Schauwecker, I.; Zarn, J.; Vasak, M. *Biochemistry* **1994**, *33*, 9699.
(12) Calderone, V.; Dolderer, B.; Hartmann, H. J.; Echner, H.; Luchinat, C.; Del Bianco, C.; Mangani, S.; Weser, U. *Proc. Natl. Acad. Sci. U.S.A.* **2005**, *102*, 51.
(13) Banci, L.; Bertini, I.; Del Conte, R.; Mangani, S.; Meyer-Klaucke, W. *Biochemistry* **2003**, *42*, 2467.
(14) Carr, H. S.; George, G. N.; Winge, D. R. *J. Biol. Chem.* **2002**, *277*, 31237.
(15) Banci, L.; Bertini, I.; Cantini, F.; Ciofi-Baffoni, S.; Gonnelli, L.; Mangani, S. *J. Biol. Chem.* **2004**, *279*, 34833.
(16) Stasser, J. P. *Biochemistry* **2005**, *44*, 3143.
(17) Stillman, M. J. *Coord. Chem. Rev.* **1995**, *144*, 461.
(18) Palumaa, P.; Kangur, L.; Voronova, A.; Sillard, R. *Biochem. J.* **2004**, *382*, 1.
(19) Bowmaker, G. A.; Clark, G. R.; Seadon, J. K.; Dance, I. G. *Polyhedron* **1984**, *3*, 535.
(20) Nicholson, J.; Abrahams, I.; Clegg, W.; Garner, C. *Inorg. Chem.* **1985**, *7*, 1092.
(21) Baumgartner, M.; Schmalle, H.; Baerlocher, C. *J. Solid State Chem.* **1993**, *107*, 63.
(22) Baumgartner, M.; Schmalle, H.; Dubler, E. *Inorg. Chim. Acta* **1993**, *208*, 135.
(23) Pavelka, M.; Simanek, M.; Sponer, J.; Burda, J. V. *J. Phys. Chem. A* **2006**, *110*, 4795.
(24) Klamt, A.; Schüürmann, G. *J. Chem. Soc., Perkin Trans. 2* **1993**, 799.
(25) Ahlrichs, R.; Bär, M.; Häser, M.; Horn, H.; Kölmel, C. *Chem. Phys. Lett.* **1989**, *162*, 165.
(26) Ahlrichs, R.; Arnim, M. *Methods and techniques in computational chemistry: METECC-95*; STEF/Club Europeen MOTECC: Cagliari, Italy, 1995.
(27) Dance, I.; Bowmaker, G.; Clark, G.; Seadon, J. *Polyhedron* **1983**, *2*, 1031.
(28) Dance, I.; Calabrese, J. *Inorg. Chim. Acta* **1976**, *19*, L41.
(29) Baumgartner, M.; Bensch, W.; Hug, P.; Dubler, E. *Inorg. Chim. Acta* **1987**, *136*, 139.
(30) Henkel, G.; Krebs, B. *Chem. Rev.* **2004**, *104*, 801.
(31) Maynard, A. T.; Covell, D. G. *J. Am. Chem. Soc.* **2001**, *123*, 1047.
(32) Enescu, M.; Jean-Philippe, R.; Pommeret, S.; Mialocq, J.-C.; Pin, S. *Phys. Chem. Chem. Phys.* **2003**, *5*, 3762.
(33) Green, A.; Presta, A.; Gasyna, Z.; Stillman, M. J. *Inorg. Chem.* **1994**, *33*, 4159.

JP8114644